



# Open Research Online

---

The Open University's repository of research publications and other research outputs

## A new method for quantifying anisotropic martensitic transformation strains accumulated during constrained cooling

### Journal Item

How to cite:

Mark, A. F.; Moat, R.; Forsey, A.; Abdolvand, H. and Withers, P. J. (2014). A new method for quantifying anisotropic martensitic transformation strains accumulated during constrained cooling. *Materials Science and Engineering: A*, 611 pp. 354–361.

For guidance on citations see [FAQs](#).

© 2014 The Authors

Version: Version of Record

Link(s) to article on publisher's website:

<http://dx.doi.org/doi:10.1016/j.msea.2014.06.012>

---

Copyright and Moral Rights for the articles on this site are retained by the individual authors and/or other copyright owners. For more information on Open Research Online's data [policy](#) on reuse of materials please consult the policies page.

---

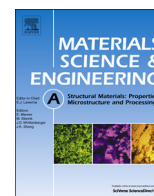
[oro.open.ac.uk](http://oro.open.ac.uk)



ELSEVIER

Contents lists available at ScienceDirect

## Materials Science &amp; Engineering A

journal homepage: [www.elsevier.com/locate/msea](http://www.elsevier.com/locate/msea)

# A new method for quantifying anisotropic martensitic transformation strains accumulated during constrained cooling

A.F. Mark<sup>a,\*</sup>, R. Moat<sup>b</sup>, A. Forsey<sup>a</sup>, H. Abdolvand<sup>a</sup>, P.J. Withers<sup>a</sup><sup>a</sup> School of Materials, University of Manchester, Manchester M13 9PL, UK<sup>b</sup> Materials Engineering, Open University, Milton Keynes MK7 6AA, UK

## ARTICLE INFO

## Article history:

Received 23 September 2013

Received in revised form

19 March 2014

Accepted 4 June 2014

Available online 12 June 2014

## Keywords:

Transformation induced plasticity

Dilatometry

Strain measurement

Finite element weld modelling

## ABSTRACT

Martensitic phase transformations during welding can play a major role in determining the final residual stresses and they can be anisotropic if the transformation occurs under stress. Traditionally, the Satoh test has been used to quantify the response, but it suffers from the fact that the temperature is not uniform along the specimen length, making it difficult to interpret the data. This shortcoming is overcome in our new experimental method using digital image correlation (DIC) to quantify the temperature dependent evolution of the transformation strain locally both parallel and perpendicular to an applied load, in this case for a high-strength low alloy (HSLA) steel and a tough, low transformation temperature weld consumable designed to mitigate tensile weld residual stresses. The method is able to separate the volumetric component of the transformation strain from the deviatoric transformation plasticity component. The volumetric component is shown to be independent of applied load, while the deviatoric component varies approximately linearly with applied load. For the HSLA steel studied here the method also reveals that the transformation start temperature rises under both tensile and compressive loading, confirming previous work. From a weld modelling viewpoint our method provides sufficient information to include the stress dependency of the anisotropic transformation strain in numerical finite element models of the weld process.

© 2014 The Authors. Published by Elsevier B.V. This is an open access article under the CC BY license (<http://creativecommons.org/licenses/by/3.0/>).

## 1. Introduction

The martensitic transformation can have a marked effect on the residual stress introduced by welding [1]. This is because the volume expansion associated with the transformation can counter the thermal contraction strains to mitigate the generation of tensile weld stresses. In fact if the transformation temperature is sufficiently low, compressive stresses can even be introduced [2] meaning that by controlling the transformation considerable control can be exerted over the weld stresses [3].

The strain associated with the martensitic transformation of a domain is a dilation normal to an invariant plane plus a shear parallel to the plane. The accommodation of the martensitic transformation of a domain within a matrix of austenite is associated with considerable local residual stresses both in the newly formed martensite and the surrounding austenite. For an essentially isotropic austenitic polycrystal, if the martensite forms (during cooling) under zero applied load all possible variants occur with equal probability such that the shear strains effectively cancel

each other giving rise to an isotropic volume expansion [4,5], see Fig. 1b.

If the transformation occurs while an externally applied load is present the net transformation strain becomes anisotropic. This can occur by a number of mechanisms, including the Magee mechanism [6], whereby specific variants are energetically preferred as in Fig. 1c. Here while the net effect appears to be a 'plastic' extension under the applied load the extension need not involve any plasticity. Alternatively the introduction of local residual stresses in the soft austenite phase can mean that even a load well below the normal yield stress may be sufficient to cause local yielding under the Greenwood and Johnson mechanism [7].

While the mechanism that causes the transformation plasticity strain is often unclear, numerical weld models of materials undergoing the martensite transformation must include it to be accurate. In the past the effect has been quantified experimentally by Satoh tests [8,9] or dilatometer tests [4].

In the Satoh test a specimen is placed in a rigid frame and heated and then cooled in a thermal treatment designed to mimic a welding cycle. The strain in the specimen is controlled by the rigid frame and the stress is measured throughout the test using a load cell in series with the specimen. The total stress caused by the

\* Corresponding author.

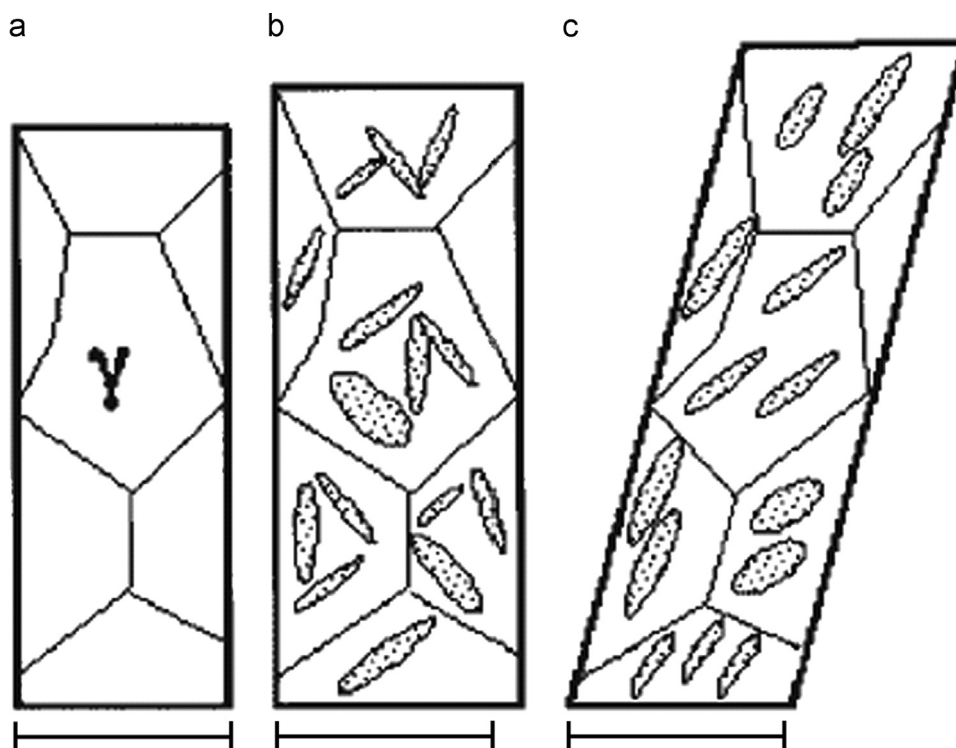


**Fig. 1.** Schematic of a polycrystalline specimen of austenite, (a) untransformed, (b) after partial transformation by a displacive mechanism into a random set of plates of ferrite, and (c) after partial transformation by displacive mechanism into an organised set of plates of ferrite. Taken from [1].

thermal expansion and contraction and by phase transformations during the thermal cycle is measured in one direction. One of the problems with the test is that the whole of the tensile specimen is not maintained at a uniform temperature so that the extent of transformation varies along the specimen length, making results difficult to interpret. While this can be obviated by using complex test-pieces [10], the test only measures the axial response.

Dilatometer tests [4] are frequently done in pairs, cooling from just above the transformation temperature on cooling,  $M_s$ . In one test the specimen bears no load, in the other it bears a load significantly below the normal yield stress at that temperature. In both cases the length change of the specimen is measured throughout the test. From these two tests the transformation plasticity strain in the loading direction can be determined, assuming the strain during transformation under zero load is isotropic.

Here a new method is described capable of measuring the strain in two directions during free and loaded tests. This allows verification of the assumption of isotropic strain under no load conditions. It also allows calculation of the deviatoric and volumetric components of strain and the instantaneous strain ratio throughout the test. This gives a more detailed picture of the transformation and its dependency on constraint than traditional tests and provides a convenient way of obtaining a representative constitutive law for finite element modelling of the transforming weld metal. In this exemplar study two materials were examined, one showing a large dependency of the transformation strain on stress and the other less so.

## 2. Experimental method

In essence, a test specimen is subjected to heating and loading in the same way as for a dilatometer test, while simultaneously the gauge section is imaged for strain measurements in the loading and transverse directions using digital image correlation.

**Table 1**

Compositions of materials examined, wt% (balance Fe).

	C	Si	Cr	Mo	V	Ni	Mn
Alloy1	0.3	0.6	3.15	1.6	0.1		
Alloy2	0.01	0.76	12.7	0.1		5.2	1.4

### 2.1. Materials

To demonstrate the method, the behaviours of two materials were studied having differing transformation temperatures and showing differing propensities for transformation plasticity. Alloy1 is a high strength, low alloy Cr–Mo steel generally used for high-strength, weight-sensitive rotating components. Alloy2 is a tough, low carbon steel, used as a weld-filler metal in stainless steel welds with strict strength, toughness and environmentally-assisted cracking resistance requirements. Their compositions are given in Table 1. Alloy1 has a conventional (high)  $M_s$ , while Alloy2 was specifically developed to have a low transformation temperature so as to mitigate tensile weld residual stresses [2]. Generally,  $M_s$  is dependent on applied load [12], but previous observations of Alloy2, showed that  $M_s$  was not greatly affected by an applied load with little evidence of variant selection in the final welds. Nevertheless, texture measurements carried out during cooling indicated that some variant selection might have occurred in the early stages of transformation [11]. Given the different transformation temperatures and different transformation responses these two alloys were identified as good candidates to demonstrate the new method for characterising transformation strain as a function of applied load.

### 2.2. Electro-thermal mechanical tester

An electro-thermal mechanical tester (ETMT) allows simultaneous variation of both temperature and applied load. The copper

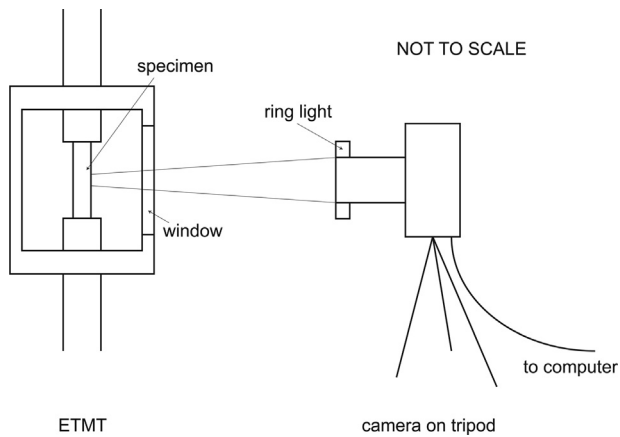


**Fig. 2.** Schematic of experimental set-up showing specimen in ETMT grips in chamber and camera on tripod. A ring light was mounted around the camera lens with the light directed at the specimen.

sample grips serve as electrical contacts for resistive heating of the specimen and, being water-cooled internally, also accelerate sample cooling.

Sub-size tensile bars ( $1.5 \times 1.5 \text{ mm}^2$  cross-section, 15 mm gauge length) of the experimental materials were cut by wire electro-discharge machining. Prior to testing, one surface was roughened by light, randomly-directed rubbing with two grades of grit paper (P400, P600) to provide suitable contrast for the digital image correlation (DIC).

In the ETMT, the temperature profile along the specimen is parabolic so that only the central 0.5 mm of the gauge length is within  $\pm 0.5 \text{ }^\circ\text{C}$  of the peak temperature. A k-type thermocouple ( $\pm 2 \text{ }^\circ\text{C}$  accuracy) was spot-welded to the centre of the gauge length, on one side. The specimen was mounted in the grips of the ETMT, using a jig to ensure it was centred and vertical. The tests were performed in an argon atmosphere to minimise surface oxidation. This meant that the specimen was enclosed in a chamber during the test and viewed through a window, see Fig. 2.

### 2.3. Digital image correlation

Digital image correlation (DIC) is well suited to mapping the strains over the hottest part of the sample. Not only can it measure strain over small areas ( $< 1 \text{ mm}^2$ ), it can provide the axial and transverse strains. A high resolution camera (VC Imager Pro 4 M from LaVision) was placed in front of the ETMT and adjusted to image the mid-length region of interest ( $0.5 \times 0.5 \text{ mm}^2$ ) of the specimen. Test images were taken while the focus was adjusted to ensure even focus across the specimen. No filtering or coloured lighting was used since the thermal regime of interest was below the temperature ( $\sim 530 \text{ }^\circ\text{C}$ ) where such measures have been found necessary [13].

A series of images of the surface of the specimen was taken throughout each thermal cycle, at a frequency of 2 Hz and subsequently processed using DaVis 7.2 from LaVision GmbH. The DIC process by which image sequences are correlated to produce a series of displacement maps is described in detail by Quinta de Fonseca et al. [14]. These maps are then differentiated to give a series of strain maps for the longitudinal and transverse strains. A typical displacement uncertainty of 0.01 pixels over the  $16 \times 16$  pixel sub-region size corresponds to a strain uncertainty of around  $\pm 0.0006$  [14].

### 2.4. Temperature and loading cycles

The specimens were heated at  $10 \text{ }^\circ\text{C/s}$  to  $950 \text{ }^\circ\text{C}$  and held for 10 s, before cooling at  $10 \text{ }^\circ\text{C/s}$  to  $470 \text{ }^\circ\text{C}$  (Alloy1) or  $450 \text{ }^\circ\text{C}$  (Alloy2)

and held for 5 s; at this point the load was applied. The specimens were then cooled at  $10 \text{ }^\circ\text{C/s}$ , with the load applied, to room temperature when the load was removed. The loads used were equivalent to applied stresses of 0, 50, and 100 MPa in tension and 50 MPa in compression.

## 3. Results

### 3.1. Alloy1 study

The strains recorded in both directions during cooling are shown in Fig. 3 for both the unloaded and loaded cases. The strains represent an average over an area of  $0.5 \times 0.5 \text{ mm}^2$  located at the centre of the specimen. As one would expect, the axial and transverse strains are similar for the unloaded case, the small difference probably being attributable to anisotropy in the starting austenitic microstructure. The difference in thermal expansion coefficient between austenite and martensite is clear from the different slopes of the linear portions of the curve before and after transformation. The effect of loading on the anisotropic development of strain during transformation is evident from the difference in the amount of expansion between  $350 \text{ }^\circ\text{C}$  and  $250 \text{ }^\circ\text{C}$ , in both directions, for the unloaded and loaded cases. It is also noteworthy that the application of load has raised the start temperature of transformation (see also Fig. 10, below).

The instantaneous strain ratio during cooling and transformation is shown in Fig. 4. The straight line in the plots represents a 1:1 ratio of transverse strain to parallel strain (i.e. isotropic strain).

The evolution of the volumetric and deviatoric components of strain throughout the transformation, adjusted for CTE effects

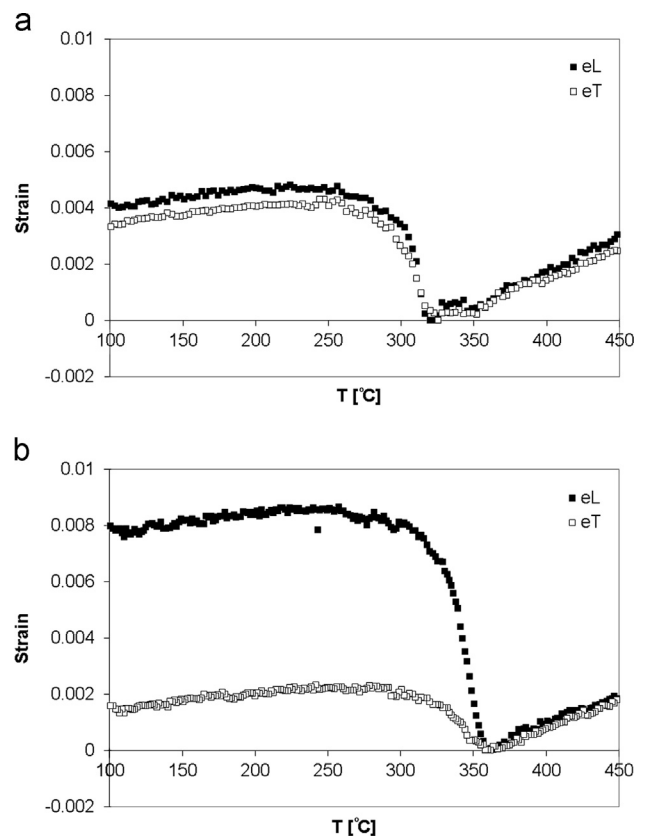


**Fig. 3.** Development of strain during cooling both parallel (filled) and transverse (open symbols) to the loading direction for Alloy1 for (a) no applied load and (b) 100 MPa applied tensile load.

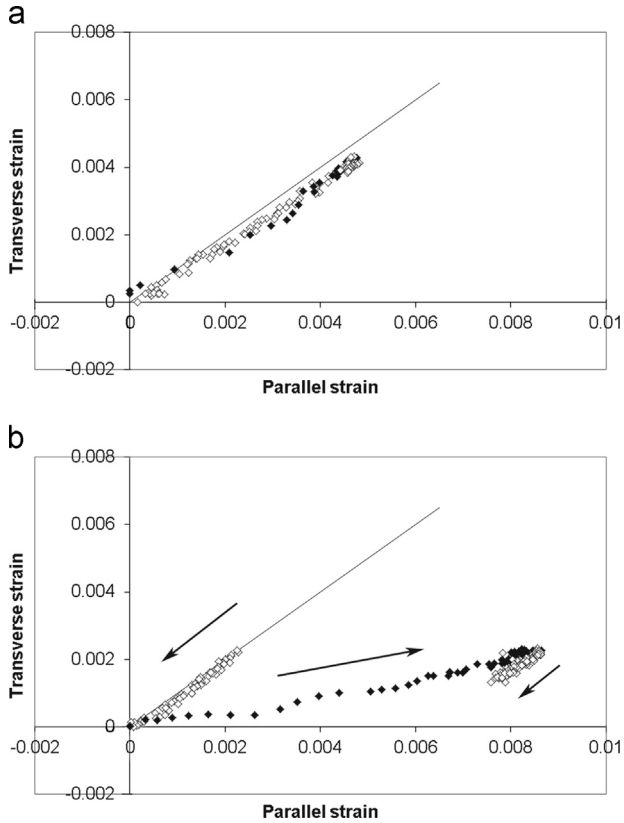


**Fig. 4.** Transverse versus parallel strain during cooling for Alloy1 for (a) no applied load and (b) 100 MPa applied tensile load. The gradient at any point represents the instantaneous strain ratio, with the straight line indicating a ratio of 1. Arrows indicate the ‘direction’ of strain changes during cooling and, for further clarity, open and closed symbols are used for decreasing and increasing strain respectively.

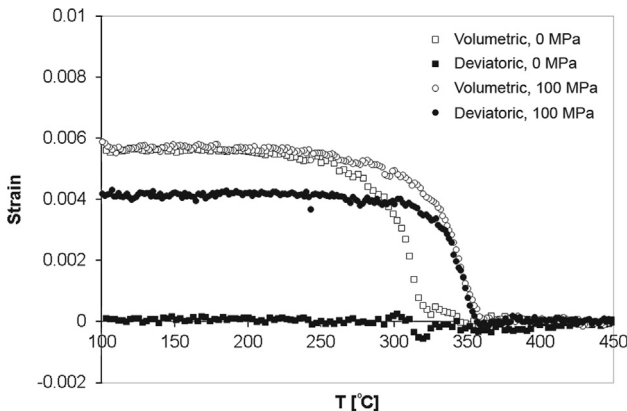


**Fig. 5.** Volumetric ( $1/3\Delta\epsilon_{vol}$ ) and deviatoric ( $\Delta\epsilon_{dev}$ ) components of the transformation strain for Alloy1. The thermal strain has been subtracted as discussed in Analysis, below.

using the rule of mixtures as discussed in the Analysis section, below, is shown in Fig. 5.

### 3.2. Alloy2 study

The strains recorded in both directions during cooling are shown in Fig. 6 for both the unloaded and loaded cases. The marked effect of loading on the strain accumulated during transformation is clear from the difference in the degree of expansion between 200 °C and 150 °C, in both directions, between the two plots.

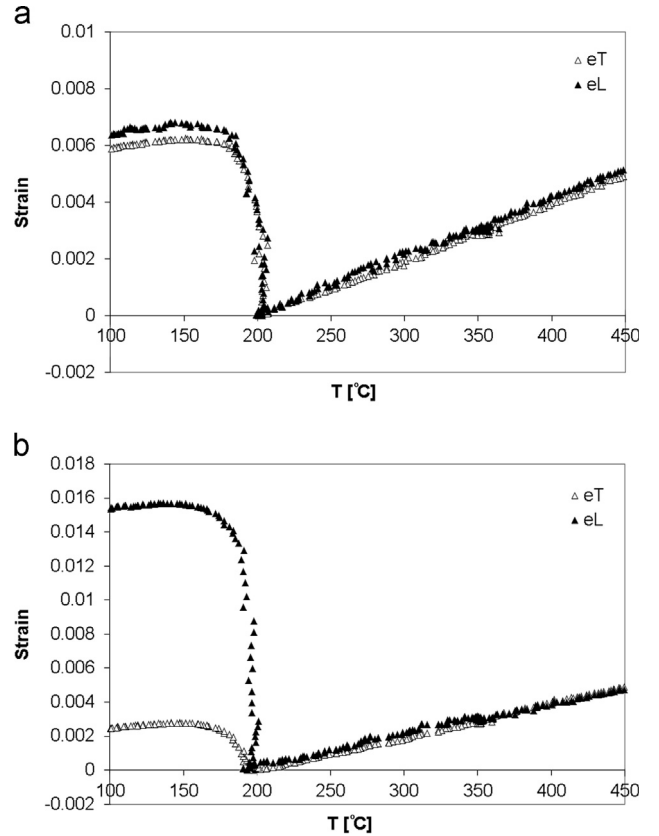


**Fig. 6.** Development of strain during cooling both parallel (filled) and transverse (open symbols) to the loading direction for Alloy2 for (a) no applied load and (b) 100 MPa applied tensile load. Note the different strain (y-axis) scale in (b).

The instantaneous strain ratio during cooling and transformation is shown in Fig. 7.

The evolution of the volumetric and deviatoric components of strain throughout transformation for Alloy2, adjusted for CTE effects as for Alloy1, is shown in Fig. 8.

## 4. Analysis

From a micromechanics viewpoint, the strain during transformation can be considered as a sum of various components:

$$\epsilon = \epsilon^e + \epsilon^p + \epsilon^{GJ} + \epsilon^{tr} + \epsilon^{\Delta T} \quad (1)$$

where  $\epsilon$ ,  $\epsilon^e$ , and  $\epsilon^p$  are the total, elastic (proportional to the applied load), and plastic strains.  $\epsilon^{GJ}$  is the strain due to the Greenwood and Johnson mechanism,  $\epsilon^{tr}$  is the strain due solely to the transformation of austenite to martensite, that is the stress-free transformation strain and the elastic accommodation of that strain in the matrix (i.e. the McGee mechanism), and  $\epsilon^{\Delta T}$  is the strain due to thermal expansion.

In Eq. (1):

$\epsilon^e$  and  $\epsilon^p$  are constant through the transformation as the load is fixed and macroscopic plasticity cannot occur since the load is below the yield stress of the material.

$\epsilon^{GJ}$  contributes solely to the deviatoric component of strain.  $\epsilon^{tr}$  can be written  $\sum f_v \epsilon_v^{tr}$  where  $f_v$  is the fraction of, and  $\epsilon_v^{tr}$  the strain from, each transforming variant. The strain is summed over all variants. If there are no preferred variants then this term is solely volumetric; if variant selection occurs then it has both volumetric and deviatoric components.

$\epsilon^{\Delta T}$  is solely volumetric but is different for the two phases.



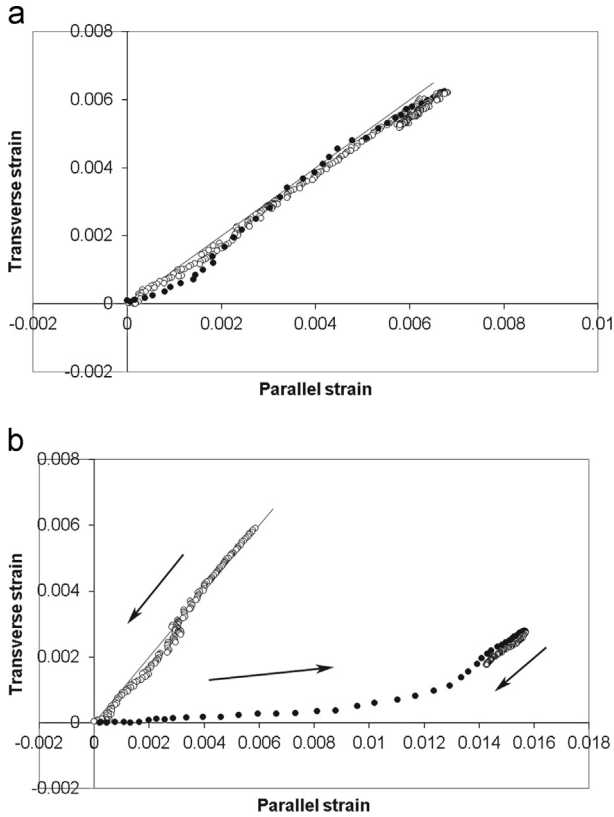


**Fig. 7.** Transverse versus parallel strain during cooling for Alloy2 for (a) no applied load and (b) 100 MPa applied tensile load. Note the different parallel strain (x-axis) scale in (b). The gradient at any point represents the instantaneous strain ratio, with the straight line indicating a ratio of 1. Arrows indicate ‘direction’ of strain changes during cooling and, for further clarity, open and closed symbols are used for decreasing and increasing strain respectively.

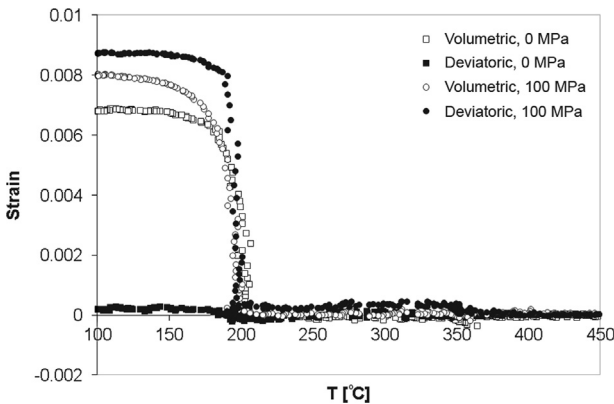


**Fig. 8.** Volumetric ( $1/3\Delta\epsilon_{vol}$ ) and deviatoric ( $\Delta\epsilon_{dev}$ ) components of the transformation strain for Alloy2. The thermal strain has been subtracted as discussed in Analysis, below.

From an empirical modelling (constitutive equation) viewpoint, the strain change during the transformation parallel ( $\Delta\epsilon_{33}$ ) and transverse ( $\Delta\epsilon_{11} = \Delta\epsilon_{22}$ ) to the loading direction can be written:

$$\Delta\epsilon_{33} = 1/3\Delta\epsilon_{vol} + \Delta\epsilon_{dev} \tag{2a}$$

$$\Delta\epsilon_{11} = 1/3\Delta\epsilon_{vol} - 0.5\Delta\epsilon_{dev} \tag{2b}$$

The contribution of the thermal expansion to the volumetric strain during the transformation can be determined using coefficients of thermal expansion (CTE) determined from the linear portions of the strain curve before and after transformation. The CTE for austenite and martensite differ, so the rule of mixtures is

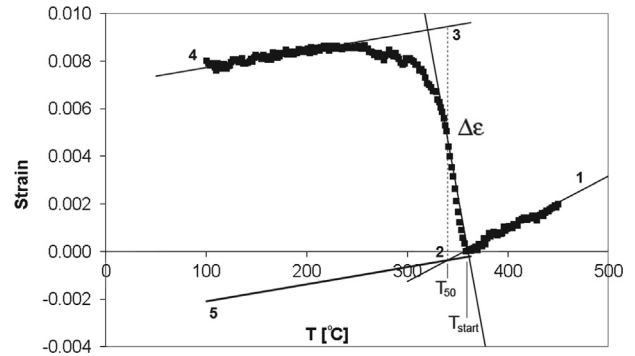


**Fig. 9.** Schematic showing how the strain change during transformation,  $\Delta\epsilon$ , was determined, in this case for Alloy2.  $T_{50}$  is the temperature at which 50% of the transformation has occurred.

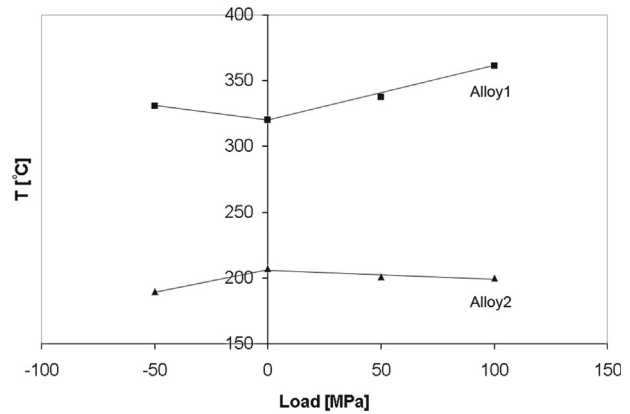


**Fig. 10.** Transformation start temperature at various loads for Alloy1 (squares) and Alloy2 (triangles). Lines are guides to the eye.

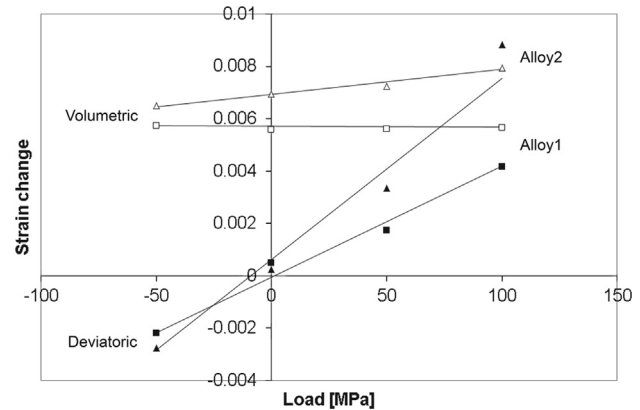


**Fig. 11.** Volumetric ( $1/3\Delta\epsilon_{vol}$ ) (open symbols) and deviatoric ( $\Delta\epsilon_{dev}$ ) (closed symbols) components of the strain change at various loads for Alloy1 (squares) and Alloy2 (triangles). Lines are guides to the eye.

often used, giving  $\Delta\epsilon^{\Delta T} = (f_M CTE_M + (1 - f_M) CTE_A) \Delta T$ . The only remaining volumetric contribution arises solely from the volume expansion from the transformation. The deviatoric strain arises from preferred orientation (Magee) and local plasticity in the austenite (Greenwood and Johnson).

The strain change during transformation,  $\Delta\epsilon$ , was determined from the measured data as shown in Fig. 9. If the transformation was instantaneous (at  $T_{50}$ , for example) and caused no strain the measured strain change with temperature would follow the path 1–2–5, with a change in slope at 2 (at  $T_{50}$ ) due to the change in thermal expansion coefficient. The effect of the strain during

transformation is to shift the curve to 3–4 instead of 2–5. The strain during transformation is here defined as the vertical distance between the two parallel lines (2–5 and 3–4) at the temperature at which the transformation is 50% complete ( $T_{50}$ ).

The start temperature for the transformation ( $T_{\text{start}}$ , see Fig. 9) was taken as the temperature of the intersection of the linear best fit lines for strain evolution prior to and during transformation.

The effect of load on start temperature for the transformation for both alloys is shown graphically in Fig. 10.

The effect of load on transformation start temperature is greater in Alloy1 than in Alloy2. The effect of load on the volumetric and deviatoric components of the strain change during transformation is shown graphically in Fig. 11.

## 5. Discussion

The data from these tests provide a much fuller picture of the transformation than obtained from conventional Satoh or dilatometer tests. Unlike the Satoh test, which provides the average response across a sample having non uniform temperature and hence a variation in transformation strain along the length, the use of DIC provides the local strain changes at the point of interest, i.e. that at which the thermocouple is placed. Further, in contrast to existing methods, our method provides the variation of both the volumetric and the deviatoric component of strain with increasing applied load. This dependency can easily be incorporated in the constitutive relations used in finite element weld models.

Unsurprisingly, the results show that for both alloys the strains in the two directions are approximately equal in the absence of applied load, i.e. the net effect is dilatational as the individual deviatoric components associated with each transforming region cancel out.

### 5.1. Dependence of start temperature on applied load

The start temperature for the transformation is more than 100 °C lower for Alloy2 than for Alloy1, which is consistent with Ms temperatures calculated on the basis of composition, for example using Andrews' linear equation [15]. It is noteworthy from Fig. 10 that the start temperature for Alloy2 is largely unaffected by the load while that for Alloy1 increases by as much as 40 °C on increasing the constraint. The results for Alloy1 are in accordance with the predictions of Patel and Cohen [16] who calculated that a tensile load will increase the start temperature proportionally to the load, as will a compressive load to a lesser extent. Assuming that the transformation begins when the driving energy exceeds a certain value, Patel and Cohen calculated the contribution to the driving energy from work done by the applied load. The difference in the effect of tensile and compressive loads arises when resolving the applied load into normal and shear forces on the transforming crystallite.

### 5.2. Dependence of volumetric strain on applied load

The volumetric component of strain is larger for Alloy2 (i.e. that with the lower transformation temperature) than for Alloy1 across the whole load range. For Alloy2 it increases slightly with increasing tensile load, while for Alloy1 it is essentially independent of load (see Fig. 11). This indicates that the volumetric component of the transformation strain is only a weak function of the applied load and can either be neglected or modelled by a linear function increasing in tension and decreasing in compression.

### 5.3. Dependence of deviatoric strain on applied load

In contrast to the volumetric component, the deviatoric component of strain is strongly dependent on the applied load, increasing essentially linearly over the load range studied, despite the fact that the loads are significantly below those necessary to cause macroscopic plasticity when the transformation is not taking place. Alloy2 shows a greater dependency on load than Alloy1 (see Fig. 11). From these results alone it is not possible to assign this effect either to variant selection (Magee) or to local plasticity (Greenwood and Johnson), or some combination of the two. Measurements of pre- and post-transformation texture might give an indication of the extent of the variant selection, allowing separation of the strains from the two mechanisms.

For weld finite element modelling of the strains associated with the transformation, it is not necessary to know whether the Magee or the Greenwood and Johnson mechanism is operating. It is sufficient to have a constitutive law that describes the anisotropy of the strain associated with the transformation. A satisfactory model would be a linear increase in the deviatoric component of strain with load.

### 5.4. Evolution of the ratio of deviatoric to dilatational strain with loading

The instantaneous strain curves of Figs. 4 and 7 provide some interesting insights. Unsurprisingly, prior and subsequent to the transformation the gradient is -1, consistent with volumetric contraction. During the transformation, however, the strain ratio changes greatly; most obviously, it reverses in sign. If the transformation occurred in a consistent manner throughout, a constant ratio of value predictable from the data in Tables 2 and 3 would be expected. In the absence of load a gradient of +1 is seen for both alloys, indicative of volumetric expansion brought about by the phase transformation. The response of Alloy1 under an applied load shows an essentially linear strain ratio (Fig. 4b) during the transformation, with axial and transverse strain changes of 0.0085 and 0.0022 respectively. Subtracting off the thermal contraction strain gives strains of 0.0101 and 0.0038 respectively. This gives a strain ratio of 0.38, which compares well with the value of 0.37 obtained from Table 2. This suggests consistency in the transformation mechanisms and is supported by Fig. 5, which shows smooth strain evolution and an essentially fixed ratio between the volumetric and dilatational components during most of the transformation.

The strain changes during the transformation of Alloy2 (Fig. 7b) are markedly different. Initially the slope of the strain ratio in Fig. 7b is very low (strain ratio  $\sim 0.07$ ) but then it rises toward a value of +1 in the later part of the transformation. This suggests that initially the transformation is highly anisotropic, being heavily biased towards the axial direction. Towards the latter stages of the transformation a gradient closer to +1 is indicative of a primarily volumetric (isotropic) transformation, which could only occur if there is negligible transformation plasticity. This is evident from Fig. 8 which shows the deviatoric strain initially increasing rapidly,

**Table 2**  
Transformation strain values for Alloy1.

	$T_{\text{start}}$	$\Delta\epsilon_{33}$	$\Delta\epsilon_{11}$	$1/3\Delta\epsilon_{\text{vol}}$	$\Delta\epsilon_{\text{dev}}$
100 MPa	361	0.0098	0.0036	0.0057	0.0042
50 MPa	337	0.0074	0.0047	0.0056	0.0017
0 MPa	320	0.0061	0.0053	0.0056	0.0005
-50 MPa	331	0.0036	0.0068	0.0057	-0.0022

**Table 3**  
Transformation strain values for Alloy2.

	$T_{\text{start}}$	$\Delta\epsilon_{33}$	$\Delta\epsilon_{11}$	$1/3\Delta\epsilon_{\text{vol}}$	$\Delta\epsilon_{\text{dev}}$
100 MPa	200	0.0168	0.0035	0.0079	0.0088
50 MPa	201	0.0106	0.0056	0.0073	0.0033
0 MPa	207	0.0072	0.0068	0.0069	0.0003
–50 MPa	190	0.0037	0.0079	0.0065	–0.0028

and then levelling off towards the end of the transformation, while the volumetric strain continues to increase significantly.

It is interesting to speculate why the transformation is anisotropic in the early stages of cooling but becomes more isotropic towards the end. One might speculate that variant selection has a greater effect at the beginning of transformation, whereas towards the end the favoured variants are exhausted. This conclusion is corroborated by a tendency for variant selection only during the initial stages of the transformation that has been noted previously during synchrotron X-ray studies of cooling [11]. Alternatively, the effect could be due to a decrease in local plasticity (Greenwood and Johnson) as the transformation proceeds due to the lower temperature (higher austenite yield strength) and/or local work hardening.

In Alloy1 the ratio indicates that transformation plasticity occurs consistently through the transformation. Since the volumetric strain component for Alloy1 is smaller it is possible the transformation does not go to completion, meaning favoured variants are not exhausted. Also, the transformation happens at higher temperature so a lower austenite yield strength might allow local plasticity to occur through the transformation.

The trends in the strain ratios for the other load cases bear out the observations above. In order to unambiguously separate the anisotropic strains arising from the Magee and Greenwood and Johnson mechanisms during the transformation in-situ texture measurements, for example by synchrotron diffraction, would be required. This is a direction of future work for this group.

### 5.5. Application of the experimental results to finite element modelling

In finite element models of the transformation on cooling the strain is generally considered in terms of volumetric and deviatoric components. The volumetric component is driven by the temperature change; thermal expansion occurs and there is a volume change due to the transformation that occurs on cooling, regardless of any applied stress. The deviatoric strain component arises from transformation plasticity contributions, either from the Greenwood and Johnson mechanism or from variant selection or both. In modelling convention the strain is expressed as a sum of thermal and transformation plasticity components:

$$\epsilon = \epsilon^{th} + \epsilon^{tr} \quad (3)$$

where  $\epsilon^{th}$  is the volumetric component and  $\epsilon^{tr}$  is the deviatoric component.

Different functions have been proposed to include  $\epsilon^{tr}$  in finite element modelling; in most cases it is expressed as [17]:

$$\epsilon^{tr} = K\dot{\zeta}\Phi(\zeta)S_{dev} \quad (4)$$

where  $K$  is a constant,  $\zeta$  is the new phase fraction,  $\dot{\zeta}$  is the rate of phase transformation and  $\Phi(\zeta)$  is a function normalised so  $\Phi(0)=0$  and  $\Phi(1)=1$ .  $S_{dev}$  is the deviatoric part of the applied stress. In Eq. (4) the deviatoric component of strain is a linear function of the applied stress; this is confirmed in our experiments, as shown in Fig. 11. The data can be used to calculate the constant,  $K$ , and,

since the strains are measured during the transformation process, the data can also be used to define  $\Phi(\zeta)$ .

Considering  $\epsilon^{tr}$ , most models assume the volumetric part of the strain is constant and is not a function of the applied load, which is also confirmed in our experiment. Hence, using the proposed technique one can identify most of the parameters required for finite element simulations.

## 6. Conclusions

A new method has been introduced for measuring strain associated with martensitic transformations during cooling. Through digital image correlation, the method gives not only the axial strains but also the transverse strains. The extra information this provides allows the calculation of the volumetric and deviatoric components of the strain throughout cooling.

The method has been demonstrated that the transformation start temperature for Alloy2 is considerably lower than that for Alloy1, and it does not change with applied load. The start temperature for Alloy1 follows the energy-based predictions of Patel and Cohen [16] in that it increases with applied load, to a larger extent for tension than compression. Further, it has been shown that the volumetric component of strain is largely independent of the applied load, while the deviatoric component varies essentially linearly. The deviatoric component is also larger for Alloy2 than for Alloy1.

The new method also allows one to follow the deviatoric and volumetric components of the transformation strain as a function of temperature. In this work, for Alloy1 the ratio of deviatoric strain to volumetric strain remains essentially constant during cooling, whereas for Alloy2 the transformation is initially very anisotropic, becoming nearly isotropic towards the end of transformation. Previous in-situ measurements by synchrotron diffraction during cooling [11] have seen variant selection during the initial stage of cooling changing to a random selection of variants as the transformation completes.

Our new method provides sufficient information to incorporate the stress dependency of the anisotropic transformation strain into numerical (finite element) models in cases where the transformation occurs, for example in weld modelling. This anisotropy in transformation strain with increasing applied load is often neglected in finite element models. From a modelling viewpoint it is not important whether the transformation plasticity is due to the Magee mechanism (variant selection) or the Greenwood and Johnson mechanism. However, since clearly further understanding of the mechanisms is of interest, future work will include pre- and post-transformation texture measurements and in-situ texture and diffraction peak profile measurements to tease out the contributions of variant selection and local plasticity to the deviatoric strain component.

## Acknowledgements

The authors would like to thank Dr. Ben Grant for his help in getting the most out of the ETMT and the DIC equipment. This research was supported by the EPSRC through grants GR/S62840/01 and EP/G042772/1. Access to the underlying research materials can be obtained by contacting AFM.

## References

- [1] P.J. Withers, H.K.D.H. Bhadeshia, *Mater. Sci. Technol.* 17 (2001) 366.
- [2] J.A. Francis, H.J. Stone, S. Kundu, R.B. Rogge, H.K.D.H. Bhadeshia, P.J. Withers, L. Karlsson, *J. Press. Vessels Tech.* 131 (2009) 041401.



- [3] R.J. Moat, H.J. Stone, A.A. Shirzadi, J.A. Francis, S. Kundu, A.F. Mark, H.K.D.H. Bhadeshia, L. Karlsson, P.J. Withers, *Sci. Technol. Weld. Join.* 16 (2011) 279.
- [4] L. Taleb, N. Cavallo, F. Waeckel, *Int. J. Plast.* 17 (2001) 1.
- [5] H.K.D. Bhadeshia, *ISIJ Int.* 42 (2002) 1059.
- [6] C.L. Magee, The nucleation of martensite, in: V.F. Zackay, H.I. Aaronson (Eds.), *Phase Transformations*, American Society for Metals, Metals Park, Ohio, 1970.
- [7] G.W. Greenwood, R.H. Johnson, *Proc. R. Soc.* 283 (1965) 403.
- [8] K. Satoh, *Trans. Jpn. Weld. Soc.* 3 (1972) 125.
- [9] K. Satoh, *Trans. Jpn. Weld. Soc.* 3 (1972) 135.
- [10] A.A. Shirzadi, H.K.D.H. Bhadeshia, *Sci. Tech. Weld. Join.* 15 (2010) 497.
- [11] R.J. Moat, *Unpublished data*.
- [12] H.S. Yang, D.W. Suh, H.K.D.H. Bhadeshia, *ISIJ Int.* 52 (2012) 164.
- [13] B.M.B. Grant, H.J. Stone, P.J. Withers, M. Preuss, *J. Strain Anal.* 44 (2009) 263.
- [14] J. Quinta de Fonseca, P.M. Mummery, P.J. Withers, *J. Microsc.* 218 (2005) 9.
- [15] G. Krauss, *Principles of Heat Treatment of Steel*, American Society for Metals, Metals Park, Ohio, 1980.
- [16] J.R. Patel, M. Cohen, *Acta Met.* 1 (1953) 531.
- [17] J.B. Leblond, J. Devaux, *Int. J. Plast.* 5 (1989) 551.